J|A|C|S
ARTICLES

Pd-Catalyzed N-Arylation of Secondary Acyclic Amides: Catalyst Development, Scope, and Computational Study

Jacqueline D. Hicks, Alan M. Hyde,* Alberto Martinez Cuezva,[†] and Stephen L. Buchwald*

Department of Chemistry, Massachusetts Institute of Technology, 77 Massachusetts Avenue, Cambridge, Massachusetts 02139

Received June 1, 2009; E-mail: sbuchwal@mit.edu; ahyde@fas.harvard.edu

---

Abstract: We report the efficient N-arylation of acyclic secondary amides and related nucleophiles with aryl nonaflates, triflates, and chlorides. This method allows for easy variation of the aromatic component in tertiary aryl amides. A new biaryl phosphine with P-bound 3,5-(bis)trifluoromethylphenyl groups was found to be uniquely effective for this amidation. The critical aspects of the ligand were explored through synthetic, mechanistic, and computational studies. Systematic variation of the ligand revealed the importance of (1) a methoxy group on the aromatic carbon of the "top ring" *ortho* to the phosphorus and (2) two highly electron-withdrawing P-bound 3,5-(bis)trifluoromethylphenyl groups. Computational studies suggest the electron-deficient nature of the ligand is important in facilitating amide binding to the LPd(II)(Ph)(X) intermediate.

Introduction

Methods for the cross-coupling of amides with aryl halides and pseudohalides have matured to a point that they may be used to reliably prepare a wide variety of substances.[1] Advances in this area are due, in large part, to the identification of improved supporting ligands. The classic copper-mediated coupling of an amide with an aryl iodide (the Goldberg reaction) proceeds catalytically and at lower temperatures when diamine ligands are employed.[2] Efficient Pd-catalyzed coupling of amides and related nucleophiles (ureas, carbamates, sulfona-

mides) with aryl bromides[3] and aryl or vinyl sulfonates[4] has largely been accomplished by the use of xantphos or XPhos as the supporting ligand. Most recently, the use of monodentate biarylphosphines bearing a methyl or methoxy group *ortho* to the phosphorus (**L3**) has enabled the coupling of amides with heteroaryl and aryl chlorides.[5,6] A prominent limitation of all amidation methods is they are mostly restricted to primary amides or lactams; a general method for the intermolecular cross-coupling of acyclic secondary amides with aryl halides and/or pseudohalides has not yet been reported.[7−9] The large size of acyclic secondary amides,[3a] combined with their relatively low nucleophilicity (compared to amines), has made secondary amides a particularly challenging substrate class for cross-coupling.

[†] Present address: Universidad de Burgos, Burgos, Spain.

(1) For reviews, see: Ley, S. V.; Thomas, A. W. *Angew. Chem., Int. Ed.* **2003**, *42*, 5400. (b) Kunz, K.; Scholz, U.; Ganzer, D. *Synlett* **2003**, 2428. (c) Ma, D.; Cai, Q. *Acc. Chem. Res.* **2008**, *41*, 1450. (d) Jiang, L.; Buchwald, S. L. In *Metal-Catalyzed Cross-Coupling Reactions*, 2nd ed.; de Meijere, A., Diederich, F., Eds.; Wiley-VCH: Weinheim, Germany, 2004. (e) Surry, D. S.; Buchwald, S. L. *Angew. Chem., Int. Ed.* **2008**, *47*, 6338.

(2) For Cu-catalyzed reactions, see: (a) Shen, R.; Porco, J. A. *Org. Lett.* **2000**, *2*, 1333. (b) Klapars, A.; Antilla, J. C.; Huang, X.; Buchwald, S. L. *J. Am. Chem. Soc.* **2001**, *123*, 7727. (c) Klapars, A.; Huang, X.; Buchwald, S. L. *J. Am. Chem. Soc.* **2002**, *124*, 7421. (d) Jiang, L.; Job, G. E.; Klapars, A.; Buchwald, S. L. *Org. Lett.* **2003**, *5*, 3667. (e) Klapars, A.; Parris, S.; Anderson, K. W.; Buchwald, S. L. *J. Am. Chem. Soc.* **2004**, *126*, 3529. (f) Pan, X.; Cai, Q.; Ma, D. *Org. Lett.* **2004**, *6*, 1809. (g) Strieter, E. R.; Blackmond, D. G.; Buchwald, S. L. *J. Am. Chem. Soc.* **2005**, *127*, 4120. (h) Strieter, E. R.; Bhayana, B.; Buchwald, S. L. *J. Am. Chem. Soc.* **2009**, *131*, 78.

(3) For the use of xantphos, see: (a) Yin, J.; Buchwald, S. L. *Org. Lett.* **2000**, *2*, 1101. (b) Yin, J.; Buchwald, S. L. *J. Am. Chem. Soc.* **2002**, *124*, 6043. (c) Shen, Q.; Hartwig, J. F. *J. Am. Chem. Soc.* **2007**, *129*, 7734. (d) Huang, J.; Chen, Y.; King, A. O.; Dilmeghani, M.; Larsen, R. D.; Faul, M. M. *Org. Lett.* **2008**, *10*, 2609. (e) Manley, P. J.; Bilodeau, M. T. *Org. Lett.* **2004**, *6*, 2433. (f) Audisio, D.; Messaoudi, S.; Peyrat, J.-F.; Brion, J.-D.; Alami, M. *Tetrahedron Lett.* **2007**, *48*, 6928. (g) Messaoudi, S.; Audisio, D.; Brion, J.-D.; Alami, M. *Tetrahedron* **2007**, *63*, 10202. (h) Artamkina, G. A.; Sergeev, A. G.; Beletskaya, I. P. *Tetrahedron Lett.* **2001**, *42*, 4381. (i) For the use of P(*t*-Bu)₃, see: Hartwig, J. F.; Kawatsura, M.; Hauck, S. I.; Shaughnessy, K. H.; Alcazar-Roman, L. M. *J. Org. Chem.* **1999**, *64*, 5575.

(4) For the use of xantphos, see: refs 3a,b and. (a) Wallace, D. J.; Klauber, D. J.; Chen, C.; Volante, R. P. *Org. Lett.* **2003**, *5*, 4749. (b) Imbriglio, J. E.; DiRocco, D.; Raghavan, S.; Ball, R. G.; Tsou, N.; Mosley, R. T.; Tata, T. R.; Collitti, S. L. *Tetrahedron Lett.* **2008**, *49*, 4897. For the use of XPhos, see: (c) Huang, X.; Anderson, K. W.; Zim, D.; Jiang, L.; Klapars, A.; Buchwald, S. L. *J. Am. Chem. Soc.* **2003**, *125*, 6653. (d) Bhagwanth, S.; Waterson, A. G.; Adjabeng, G. M.; Hornberger, K. R. *J. Org. Chem.* **2009**, *74*, 4634. For the use of other ligands, see: (e) Klapars, A.; Campos, K. R.; Chen, C.; Volant, R. P. *Org. Lett.* **2005**, *7*, 1185. (f) Willis, M. C.; Brace, G. N.; Holmes, I. P. *Synthesis* **2005**, 3229.

(5) (a) Ikawa, T.; Barder, T. E.; Biscoe, M. R.; Buchwald, S. L. *J. Am. Chem. Soc.* **2007**, *129*, 13001. (b) Fors, B. P.; Krattiger, P.; Strieter, E.; Buchwald, S. L. *Org. Lett.* **2008**, *10*, 3505. (c) Fors, B. P.; Dooleweerdt, K.; Zeng, Q.; Buchwald, S. L. *Tetrahedron* **2009**, *65*, 6576.

(6) For additional examples of amidations with aryl chlorides, see: (a) Ghosh, A.; Sieser, J. E.; Riou, M.; Cai, W.; Rivera-Ruiz, L. *Org. Lett.* **2003**, *5*, 2207. (b) Shen, Q.; Shekhar, S.; Stambuli, J. P.; Hartwig, J. F. *Angew. Chem., Int. Ed.* **2005**, *44*, 1371. (c) Ligthart, G. B. W. L.; Ohkawa, H.; Sijbesma, R. P.; Meijer, E. W. *J. Org. Chem.* **2006**, *71*, 375. (d) Piguel, S.; Legraverend, M. *J. Org. Chem.* **2007**, *72*, 7026. (e) McLaughlin, M.; Palucki, M.; Davies, I. W. *Org. Lett.* **2006**, *8*, 3311. For an example of amidation with *gem*-dichloroolefins, see: (f) Ye, W.; Mo, J.; Zhao, T.; Xu, B. *Chem. Commun.* **2009**, 3246.
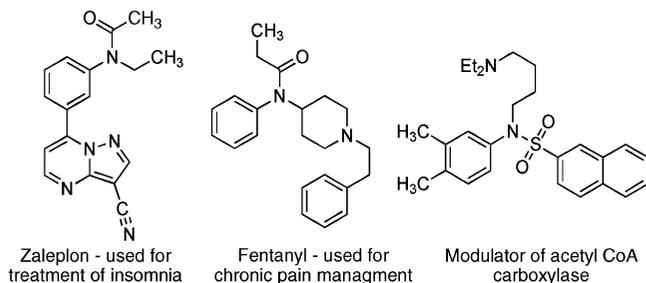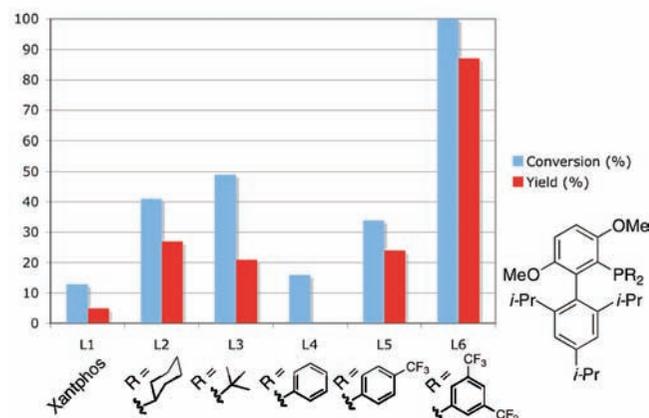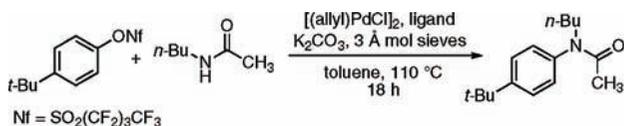
Figure 1. Representative biologically active tertiary aryl amides and sulfonamides.

Chart 1. Ligand Optimization for the Coupling of 4-*tert*-Butylphenyl Nonaflate and *N*-Butyl Acetamide[a]

[a] ArONf (1 equiv), amide (2.5 equiv), [(allyl)PdCl]$_2$ (1 mol %), ligand (5 mol %), base (2.0 equiv), 3 Å mol sieves (50 mg/mL), solvent (0.25 M), 110 °C, 18 h.

Tertiary aryl amides and sulfonamides, the primary products described in this paper, are found in a variety of biologically active molecules (Figure 1).[10] Access to this class of compounds by arylation of the secondary amides would have advantages over traditional acylation strategies because it would allow for easy variation of the aromatic component, facilitating the generation of analogues for SAR studies. Additionally, secondary amides and carbamates are often intermediates in synthetic sequences,[11] and the ability to arylate these directly would improve the efficiency of synthetic routes.

Herein, we describe the rational development of a new biaryl phosphine (JackiePhos, **L6**) with P-bound 3,5-(bis)trifluoromethylphenyl groups that facilitates amide binding by creating a more electrophilic Pd(II) intermediate. We have examined aspects of this catalyst system by synthetic, mechanistic, and computational investigations. The synthetic investigations will focus on (1) substrate scope for the cross-coupling of secondary amides with aryl triflates and nonaflates, (2) cross-coupling of related nucleophiles (ureas, carbamates, sulfonamides), (3) extension of this method to include aryl chlorides, and (4) development of a diarylation process. The mechanistic investigations will focus on (1) the correlation of ligand structure to catalyst stability and (2) trends in aryl halide reactivity and the mechanistic implications. Finally, a computational study will examine each catalytic step for a series of related ligands to understand the effect of structural substitutions.

Results

In designing a new ligand for the N-arylation of secondary amides, we took into account existing knowledge of ligand effects and the mechanism of amidation. Xantphos, the standard ligand for the amidation of aryl iodides, bromides, and triflates, was ineffective as a ligand for the reaction in Chart 1. Instead we chose to focus our efforts on ligands derived from the BrettPhos biaryl motif[12] (Chart 1), which contains two methoxy groups on the upper ring of the biaryl. This scaffold imparts properties that give catalysts superior performance in a number of C−N bond-forming transformations. Reactions employing BrettPhos[13] (**L2**) and *t*-Bu$_2$BrettPhos[5c] (**L3**) provided unsatisfactory yields of the desired product (27% and 21%, respectively). Based on our knowledge that "transmetalation" was rate-limiting for primary amides[5a] (and this step would likely be even more difficult for the larger secondary amides), we undertook the development of ligands that would facilitate this step. We hypothesized that a more electrophilic and less sterically demanding Pd(II) intermediate was necessary to facilitate amide binding. Moreover, a similar strategy was employed by Beletskaya for the N-arylation of ureas in which an electron-deficient xantphos ligand possessing P-bound 3,5-(bis)trifluoromethylphenyl groups was shown to give the most active catalyst.[13] Toward this goal we prepared ligands **L4**−**L6**, in which the P-bound alkyl groups in **L2** and **L3** were replaced with aryl groups. The strongly electron-withdrawing 3,5-(bis)trifluoromethylphenyl substituent in ligand **L6** provided the most efficient ligand, and the catalyst derived from **L6** provided the desired product in 87% yield. Consistent with our supposi-

(7) For intramolecular examples, see: (a) Wolfe, J. P.; Rennels, R. A.; Buchwald, S. L. *Tetrahedron* **1996**, *52*, 7525. (b) Wagaw, S.; Rennels, R. A.; Buchwald, S. L. *J. Am. Chem. Soc.* **1997**, *119*, 8451. (c) Yang, B. H.; Buchwald, S. L. *Org. Lett.* **1999**, *1*, 35. (d) Yamada, K.; Kubo, T.; Tokuyama, H.; Fukuyama, T. *Synlett* **2002**, 231. (e) Ooi, T.; Kameda, M.; Maruoka, K. *J. Am. Chem. Soc.* **2003**, *125*, 5139. (f) Poondra, R. R.; Turner, N. J. *Org. Lett.* **2005**, *7*, 863. (g) Bonnaterre, F.; Bois-Choussy, M.; Zhu, J. *Org. Lett.* **2006**, *8*, 4351. (h) Hoogenbrand, A.; Lange, J. H. M.; Iwema-Bakker, W. I.; Hartog, J. A. J.; Schaik, J.; Feenstra, R. W.; Terpstra, J. W. *Tetrahedron Lett.* **2006**, *47*, 4361. (i) Feng, G.; Wu, J.; Dai, W. *Tetrahedron Lett.* **2007**, *48*, 401. (j) Hoogenbrand, A.; Lange, J. H. M.; Hartog, J. A. J.; Henzen, R.; Terpstra, J. W. *Tetrahedron Lett.* **2007**, *48*, 4461. (k) Furuta, T.; Kitamura, Y.; Hashimoto, A.; Fujii, S.; Tanaka, K.; Kan, T. *Org. Lett.* **2007**, *9*, 183. (l) Kalinski, C.; Umkehrer, M.; Ross, G.; Kolb, J.; Burdack, C.; Hiller, W. *Tetrahedron Lett.* **2006**, *47*, 3423.

(8) For isolated intermolecular examples, see: refs 2c, 3a, 3b, 5a and Deng, W.; Wang, Y.-F.; Zou, Y.; Liu, L.; Guo, Q.-X. *Tetrahedron Lett.* **2004**, *45*, 2311.

(9) For secondary formamides, see: refs 2c, 3a, 3b, 4c, and 5a.

(10) (a) Wagner, J.; Wagner, M. L.; Hening, W. A. *Ann. Pharmacother.* **1998**, *36*, 680. (b) VanBever, W. F. M.; Niemegeers, C. J. E.; Janssen, P. A. J. *J. Med. Chem.* **1974**, *17*, 1047. (c) Anderson, R.; Hokama, T.; Lee, S.-F.; Oey, R.; Elich, T.; Breazeale, S. Preparation of modulators of acetyl coenzyme A carboxylase as fungicides and pharmaceuticals. U.S. Patent 20080200461, 2008.

(11) Greene, T. W.; Wuts, P. G. M. *Protective Groups in Organic Chemistry*, 3rd ed.; John Wiley & Sons: New York, 1999; pp 503−564.

(12) Fors, B. P.; Watson, D. A.; Biscoe, M. R.; Buchwald, S. L. *J. Am. Chem. Soc.* **2008**, *130*, 13552.

(13) Sergeev, A. G.; Artamkina, G. A.; Beletskaya, I. P. *Tetrahedron Lett.* **2003**, *44*, 4719.

tion, the conversion and product yields increased as the ligand became more electron-deficient (R = 3,5-CF$_3$Ph > 4-CF$_3$Ph > Ph).

Several other aspects of the reaction conditions utilized for the N-arylation of secondary amides deserve comment.[14] Aryl nonaflates (ArONf = ArOSO$_2$(CF$_2$)$_3$CF$_3$)[15] were chosen as a cross-coupling partner because they are less susceptible to hydrolysis than aryl triflates, while still providing a similar, highly electrophilic, Pd(II) intermediate.[16,17] The use of a nonpolar solvent such as toluene was found to be critical in obtaining high yields, whereas reactions in polar solvents (e.g., *t*-BuOH, DME) were less efficient. Additionally, the inclusion of molecular sieves in the reaction mixture improved the yields by inhibiting the formation of phenols and related side products.[18] The [(allyl)PdCl]$_2$ precatalyst was chosen due to its ease of use and lack of coordinating ligands (such as dba).[19] However, Pd(OAc)$_2$ could also be used if a preactivation step was employed to ensure formation of the Pd(0) complex.[5b]

Synthetic Investigations. With optimized reaction conditions in hand, we examined the scope of the method. Secondary amides coupled efficiently with a variety of electron-deficient, electron-neutral, and moderately electron-rich aryl nonaflates, with electron-deficient aryl nonaflates typically giving the highest yields (Table 1, entries 1−3). α-Branched amides reacted smoothly (entries 5 and 6), but branched alkyl substitution on the nitrogen was not tolerated. In addition to nonaflates, aryl triflates were also successfully converted to product (entries 7 and 8). In difunctionalized substrates, it was found (unsurprisingly) that the nonaflate group reacted in preference to a chloride substituent (entries 9 and 10). A relatively small group at the *ortho* position of the aryl sulfonate such as Cl was tolerated, but larger substituents were not. Acetanilide and other *N*-aryl amides are traditionally difficult substrates for Pd-catalyzed cross-coupling reactions, but by using a slight modification of our general protocol, employing K$_3$PO$_4$ as the base, acetanilide could be N-arylated in 78% yield (entry 11).[20] We note that attempts to realize the same product from the aryl bromide using xantphos as the supporting ligand gave a very low yield of the product.[21]

Given the successful coupling of secondary amides, we next examined the reaction of carbamates, ureas, and sulfonamides. Substituted ureas proved to be difficult substrates and could only

Table 1. Pd-Catalyzed Coupling of Aryl Nonaflates and Triflates with Secondary Amides[a]

entry	ArX	amide	product	yield[b]
1	R = *t*-Bu		1 R = *t*-Bu	79%
2	R = Me		2 R = Me	85%
3	R = CO$_2$Me		3 R = CO$_2$Me	87%
4				79%
5				85%
6[c]				82%
7				76%
8				77%
9				72%
10				70%
11[d]				78%

[a] Reaction conditions: ArONf/ArOTf (1 equiv), amide (2.5 equiv), [(allyl)PdCl]$_2$ (1 mol %), JackiePhos (5 mol %), K$_2$CO$_3$ (2.0 equiv), 3 Å mol sieves (200 mg/mmol), toluene (0.25 M), 110 °C, 17 h. [b] Yields reported are an average of at least two runs determined to be >95% pure by elemental analysis or ^{1}H NMR. [c] Pd(OAc)$_2$ (3 mol %), JackiePhos (7 mol %), H$_2$O activation. [d] K$_3$PO$_4$ was used instead of K$_2$CO$_3$.

be coupled with electron-deficient nonaflates, and then only in moderate yields (Table 2, entries 1 and 2). In contrast, secondary carbamates, which are less sterically demanding, were excellent substrates. The coupling of Boc- and Cbz-protected amines proceeded in 87% and 90% yield, respectively (entries 3 and 6). The use of secondary sulfonamides also provided good yields of coupled products (entries 7−9). These examples are significant because there are only isolated examples of the successful

(14) For a more complete ligand examination and condition optimization, see Supporting Information.

(15) Aryl nonaflates can be easily prepared from the corresponding phenols and nonafluorobutanesulfonyl fluoride. For their preparation and use in C−N coupling, see: (a) Anderson, K. W.; Mendez-Perez, M.; Priego, J.; Buchwald, S. L. *J. Org. Chem.* **2003**, *68*, 9563. (b) Tundel, R. E.; Anderson, K. W.; Buchwald, S. L. *J. Org. Chem.* **2006**, *71*, 430.

(16) For the use of ArONf substrates in Heck reactions, see: (a) Beletskaya, I. P.; Cheprakov, A. V. *Chem. Rev.* **2000**, *100*, 3009. (b) Lyapkalo, I. M.; Webel, M.; Reibig, H.-U. *Eur. J. Org. Chem.* **2002**, 3646.

(17) Aryl nonaflates are generally more resistant to hydrolysis than the corresponding triflates. For an example, see: (a) Zhang, X.; Sui, Z. *Tetrahedron Lett.* **2003**, *44*, 3071.

(18) Anderson, K. W.; Ikawa, T.; Tundel, R. E.; Buchwald, S. L. *J. Am. Chem. Soc.* **2006**, *128*, 10694.

(19) Coordination of dba can result in diminished reactivity. See: (a) Fairlamb, I. J. S.; Kapdi, A. R.; Lee, A. F.; McGlacken, G. P.; Weissburger, F.; de Vries, A. H. M.; Vondervoort, L. S. *Chem.—Eur. J.* **2006**, *12*, 8750. (b) Mace, Y.; Kapdi, A. R.; Fairlamb, I. J. S.; Jutand, A. *Organometallics* **2006**, *25*, 1795. (c) Amatore, C.; Jutand, A. *Coord. Chem. Rev.* **1998**, *178*, 511.

(20) For Cu-catalyzed arylations of *N*-aryl amides with aryl iodides and bromides: refs 2b, 2c, 2f and Freeman, H. S.; Butler, J. R.; Freedman, L. D. *J. Org. Chem.* **1978**, *43*, 4975.

(21) Yin, J.; Buchwald, S. L., unpublished results.

Table 2. Pd-Catalyzed Coupling of Aryl Nonaflates and Triflates with Secondary Ureas, Carbamates, and Sulfonamides[a]

entry	ArX	amide	product	yield[b]
1				64%
2				53%
3				90%
4				88%
5				86%
6				87%
7				88%
8				83%
9				87%
10				77%

[a] Reaction conditions: ArONf/ArOTf (1 equiv), urea or carbamate (2.5 equiv), [(allyl)PdCl]$_2$ (1 mol %), JackiePhos (5 mol %), K$_2$CO$_3$ (2.0 equiv), 3 Å mol sieves (50 mg/mL), toluene (0.25 M), 110 °C, 17 h. [b] Yields reported are an average of at least two runs determined to be >95% pure by elemental analysis or ^{1}H NMR.

Table 3. Pd-Catalyzed Coupling of Aryl Chlorides with Secondary Amides, Carbamates, and Sulfonamides[a]

entry	ArCl	amide	product	yield[b]
1	R = *t*-Bu		R = *t*-Bu	81%
2	R = *n*-Bu		R = *n*-Bu	76%
3				57%
4				81%
5				87%
6[c]				74%

[a] Reaction conditions: ArCl (1 equiv), amide (2.5 equiv), [(allyl)-PdCl]$_2$ (1 mol %), JackiePhos (5 mol %), base (2.0 equiv), 3 Å mol sieves (200 mg/mmol), solvent (0.25 M), 110 °C, 18 h. [b] Yields reported are an average of at least two runs determined to be >95% pure by elemental analysis or ^{1}H NMR. [c] K$_3$PO$_4$ was used instead of Cs$_2$CO$_3$.
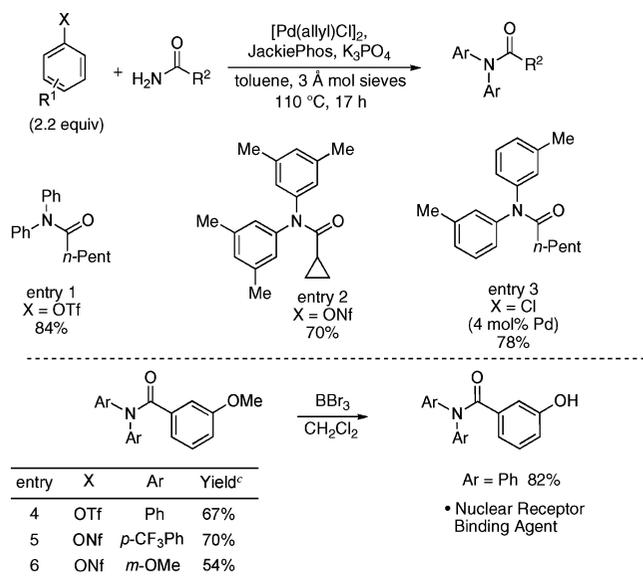
cross-coupling of *N*-alkyl carbamates[22] and, to the best of our knowledge, the intermolecular coupling of *N*-alkyl acyclic sulfonamides or *N*-alkyl, *N'*,*N'*-dialkyl ureas has not yet been reported.

To expand the utility of this method, we sought to develop conditions that would allow for the coupling of secondary amides with aryl chlorides. Many aryl chlorides are commercially available, and the ability to utilize these substrates would improve the generality of this method.[23] Increasing the reaction temperature and utilizing Cs$_2$CO$_3$ as the base provided good yields of amidation products. The substrate scope of the aryl chloride coupling was briefly examined as shown in Table 3. A variety of aryl chlorides were successfully coupled with secondary amides as well as with a secondary carbamate (entry 4) and a secondary sulfonamide (entry 5). The reaction of more hindered amides proved to be difficult with aryl chlorides; for those substrates in particular, aryl triflates/nonaflates are recommended as the coupling partners.

Given our success in coupling *N*-aryl amides with aryl nonaflates and chlorides, we examined the diarylation of a

(22) For isolated examples of N-arylation with secondary carbamates, see: refs 3a, 3c, and Tasler, S.; Mies, J.; Lang, M. *Adv. Synth. Catal.* **2007**, *349*, 2286.
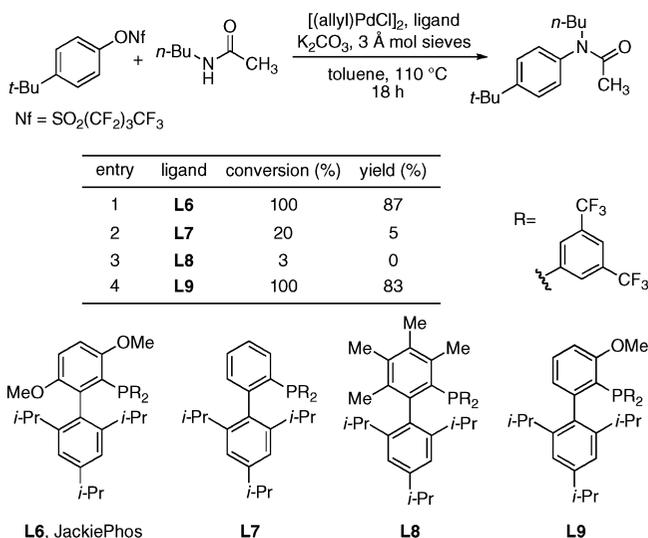
(23) (a) Littke, A. F.; Fu, G. C. *Angew. Chem., Int. Ed.* **2002**, *41*, 4176. (b) Grushin, V. V.; Alper, H. *Chem. Rev.* **1994**, *94*, 1047.

Table 4. Diarylation of Primary Amides and Synthesis of a Nuclear Receptor Binding Agent and Related Analogues[a,b]

entry 1
X = OTf
84%

entry 2
X = ONf
70%

entry 3
X = Cl
(4 mol% Pd)
78%

entry	X	Ar	Yield[c]
4	OTf	Ph	67%
5	ONf	p-CF₃Ph	70%
6	ONf	m-OMe	54%

Ar = Ph 82%
• Nuclear Receptor Binding Agent

[a] Reaction conditions: ArX (2.2 equiv), amide (1.0 equiv), [(allyl)PdCl]₂ (1 mol %), JackiePhos (5 mol %), K₃PO₄ (3.0 equiv), 3 Å mol sieves (200 mg/mmol), toluene (0.25 M), 110 °C, 17 h. [b] Yields reported are an average of at least two runs determined to be >95% pure by elemental analysis or ¹H NMR. [c] Runs conducted with [(allyl)PdCl]₂ (1.5 mol %), JackiePhos (7 mol %), 42 h.

primary amide.[24] By combining a primary amide with 2.2 equiv of aryl halide or pseudohalide and 3 equiv of base under otherwise identical reaction conditions to that described above, good yields of the desired *N,N*-diaryl amides could be obtained (Table 4). This diarylation method allows for the rapid synthesis of diaryl benzamide derivatives. These compounds exhibit interesting biological activity as nuclear receptor binding agents.[25] An example is 3-hydroxy-*N,N*-diphenylbenzamide, which alters pS2/TFF1 expression levels. (pS2/TFF1 is important in maintaining gastric mucosal integrity and may act as a tumor suppressor signal in the stomach.[26]) Through the diarylation of 3-methoxybenzamide (entries 4−6), a series of 3-hydroxy-*N,N*-diphenylbenzamide analogues were readily available.

Mechanistic Investigation. Our recent studies on C−N bond formation have shown that ligands containing methoxy groups on the upper ring of the biaryl backbone provide significantly better results than those without the substituents. To probe the importance of the methoxy groups, a series of JackiePhos analogues were prepared and tested. Ligands **L7**−**L9** (Table 5), containing variable substitution on the upper biaryl ring, were examined under standard reaction conditions for the coupling of *N*-butylacetamide and of 4-*tert*-butylphenyl nonaflate. The
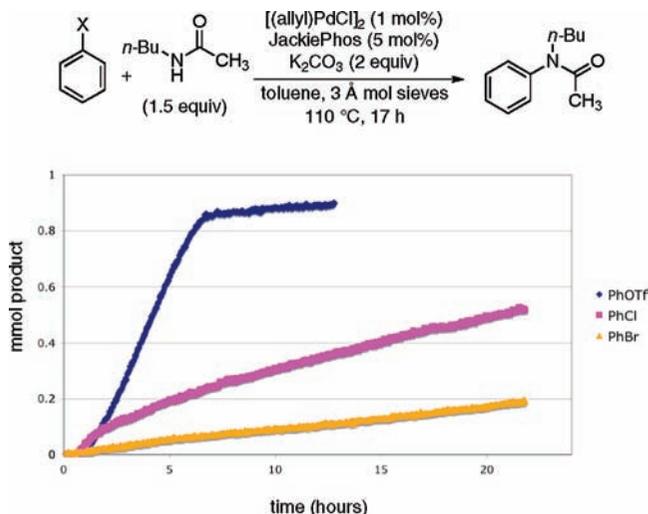
(24) For Cu-catalyzed diarylations with aryl bromides and iodides, see: (a) Hisayuki, K.; Hiroyuki, M.; Koji, H. Method for Producing Aromatic Diamine Derivative. EP 1593665, 2005. (b) Yabunouchi, N.; Kawamura, M. Aromatic Amine Derivative and Organic Electroluminescent Device Using the Same. WO2006073054, 2006. (c) Kawamura, H.; Yabunouchi, N. Aromatic Triamine Compound and Organic Electroluminescent Device Using the Same. WO2006114921, 2006.
(25) Dalton, J.; Barrett, C.; He, Y.; Hong, S.; Miller, D. D.; Mohler, M. L.; Narayanan, R.; Wu, Z. Nuclear Receptor Binding Agents. WO 2007/062230 A2, 2007.
(26) Fujii, Y.; Shimada, T.; Koike, T.; Hosaka, K.; Tabei, K.; Namatame, T.; Tajima, A.; Yoneda, M.; Terano, A.; Hiraishi, H. *Aliment Pharmacol. Ther. Symp. Ser.* **2006**, *2*, 285.

Table 5. Variation of the Upper Ring of the Biaryl Backbone

Nf = SO₂(CF₂)₃CF₃

entry	ligand	conversion (%)	yield (%)
1	**L6**	100	87
2	**L7**	20	5
3	**L8**	3	0
4	**L9**	100	83

L6, JackiePhos   L7   L8   L9

catalyst derived from ligand **L9**, containing only one methoxy substituent *ortho* to the phosphorus, led to successful amidation. Yields for amidation reactions using **L9** were similar to those obtained with JackiePhos, and monitoring the amidation with *in situ* IR indicated that the reaction profiles were nearly identical. However, the catalyst derived from ligand **L7**, lacking both of the methoxy groups, provided only 5% of the desired product and quickly degraded to palladium black. This indicates that the upper methoxy *ortho* to the phosphorus is of critical importance to catalyst stability. To determine if this was simply a steric effect, ligand **L8** containing an *ortho* methyl group was synthesized. Interestingly, **L8** was not a useful ligand for amidation reactions despite NMR experiments showing it undergoes oxidative addition to PhCl. Thus, the methoxy group *ortho* to the phosphorus of JackiePhos cannot be substituted with a slightly larger, noncoordinating group.

To better understand the relative reactivity of the aryl halide or pseudohalide in these amidation reactions, we compared the reaction profiles of phenyl triflate, iodobenzene, bromobenzene, and chlorobenzene with *N*-butyl acetamide. The reactions were monitored for product formation by *in situ* IR spectroscopy (Chart 2). The reaction of *N*-butyl acetamide with phenyl triflate proceeded to completion in just over 5 h. In contrast, the reaction of aryl halides did not reach completion in 22 h. We observed some unexpected trends in the reactions of the aryl halides; the reaction of chlorobenzene was significantly faster than that of bromobenzene, which in turn was much faster than iodobenzene, which produced essentially no product. The general trend of ArOTf/ArONf > ArCl > ArBr > ArI was also observed for the other substituted aryl halides/pseudohalides examined.

To gain a more thorough understanding of the origin of these trends, we carried out several competition experiments. In Table 6 a comparison of the yields for the cross-coupling of *N*-butyl acetamide with aryl electrophiles under the optimal reaction conditions developed for aryl chlorides is shown. The yields given in this table are consistent with the relative reactivity of this series of substrates. Given that aryl chlorides react faster under these conditions than the corresponding aryl bromides, we performed a competition experiment between 1-*n*-butyl-4-chlorobenzene and 4-bromotoluene (eq 1). As expected, exclusive cross-coupling with the 4-bromotoluene was observed, consistent with a mechanism in which oxidative addition occurs preferentially with 4-bromotoluene. A similar competition

Chart 2. Comparison of Reaction Profiles for PhOTf, PhCl, and PhBr

Table 6. Competition Experiments

entry	R	X	yield
1	CH₃	OTf	78%
2	n-Bu	Cl	77%
3	CH₃	Br	67%
4	CH₃	I	3%

experiment between 1-*n*-butyl-4-chlorobenzene and 4-iodotoluene provided no cross-coupled product (eq 2), demonstrating that oxidative addition occurred with 4-iodotoluene in preference to 1-*n*-butyl-4-chlorobenzene. These results strongly disfavor a mechanism in which oxidative addition affects the observed rate but instead are consistent with the idea that the "transmetalation" step is responsible for the observed trend in reactivity. In our previous kinetic studies on amidation, the faster rate of "transmetalation" for aryl triflates was attributed to a more labile LPd(Ph)OTf complex compared to LPd(Ph)halide complexes.[5a] Analogously, the rate of amide/amidate attack on LPd(Ph)Cl may be faster than the attack on LPd(Ph)Br due to the more electrophilic nature of palladium in LPd(Ph)Cl. This is supported

by the trend in rates of associative ligand exchange of [Pt(di-en)X]$^{n+}$ complexes, following the order Cl > Br > I.[27]

Computational Studies

Future advances in the design of biarylmonophosphine ligands would benefit from a firm understanding of the effects bestowed by substituents appended to the biaryl backbone. Although we were pleased with the superior performance of JackiePhos in comparison to other biarylmonophosphine ligands, we sought further mechanistic support for our original hypothesis that its electron-withdrawing nature allows for faster transmetalation; this prompted us to investigate the role of the structural features present in this ligand. For these studies, we chose to focus on two points: (1) determination of the effect of substitution of different P-bound R groups (i.e., 3,5-CF₃Ph, *t*-Bu, Cy, Ph) and (2) the development of an understanding of the role of the methoxy group bound to the upper ring *ortho* to the phosphorus.

Since we were unable to measure the relative rates of each mechanistic step due to difficulties in isolating catalytic intermediates, we turned instead to a computational approach using DFT methods. Computational investigations of Pd-catalyzed cross-coupling reactions have become increasingly routine, but an examination of the literature reveals that the majority of these analyses are limited to catalysts containing small phosphines (e.g., PH₃, PMe₃, H₂PCH₂CH₂PH₂) that serve as models for larger ligands (e.g., PPh₃, P(*t*-Bu)₃, Ph₂PCH₂-CH₂PPh₂).[28] While the conclusions from these studies have provided much insight into the operative mechanism of these processes, many difficult cross-coupling reactions do not proceed with these simple ligands. Therefore, caution should be exercised when applying approximations to ligands when examining such reactions.[29]

With the rapid increases in computational power and concurrent decrease in cost, we favor a more rigorous approach, which entails modeling the complete catalyst with all-atom DFT. We believe that studying the subtle structural features of the ligand is critical for a thorough mechanistic understanding. Furthermore, in the following discussion we compare several related biaryl monophosphines that behave markedly different in promoting catalysis. The direct comparison of ancillary phosphine ligands by computational methods represents an infre-
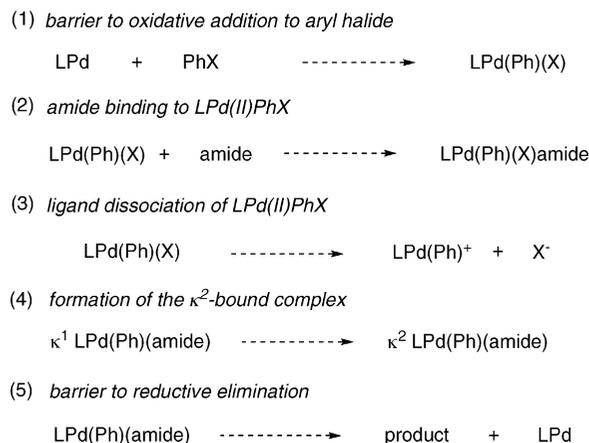
(27) Richens, D. T. *Chem. Rev.* **2005**, *105*, 1961.
(28) For representative examples, see: (a) Ariafard, A.; Lin, Z. *Organometallics* **2006**, *25*, 4030. (b) Legault, C. Y.; Garcia, Y.; Merlic, C. A.; Houk, K. N. *J. Am. Chem. Soc.* **2007**, *129*, 12664. (c) Nova, A.; Ujaque, G.; Maseras, F.; Lledós, A.; Espinet, P. *J. Am. Chem. Soc.* **2006**, *128*, 14571. (d) Álvarez, R.; Faza, O. N.; López, C. S.; de Lera, A. R. *Org. Lett.* **2006**, *8*, 35. (e) Braga, A. A. C.; Ujaque, G.; Maseras, F. *Organometallics* **2006**, *25*, 3647. (f) Ananikov, V. P.; Musaev, D. G.; Morokuma, K. *Organometallics* **2005**, *24*, 715. (g) Zuidema, E.; van Leeuwen, P. W. N. M.; Bo, C. *Organometallics* **2005**, *24*, 3703.
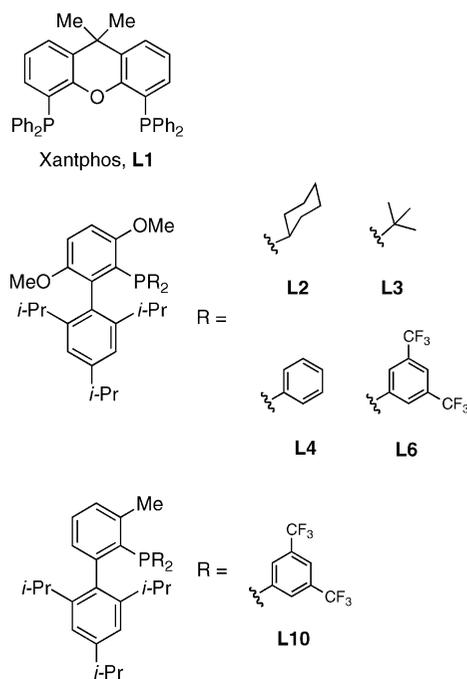(29) For examples that illustrate the importance of calculating the full ligand structure in Pd-catalyzed cross-coupling reactions, see: (a) Li, Z.; Fu, Y.; Guo, Q.; Liu, L. *Organometallics* **2008**, *27*, 4043. (b) Barder, T. E.; Biscoe, M. R.; Buchwald, S. L. *Organometallics* **2007**, *26*, 2183.
(30) For the calculated effect of ligand structure on the barrier to oxidative addition of aryl halides with LnPd(0), see ref 28a and (a) Kozuch, S.; Amatore, C.; Jutand, A.; Shaik, S. *Organometallics* **2005**, *24*, 2319. For the effect on the overall cycle of a Pd-catalyzed Suzuki−Miyuara coupling, see: (b) Huang, Y.; Weng, C.; Hong, F. *Chem.−Eur. J.* **2008**, *14*, 4426. For the effect on the barrier to reductive elimination of LnPd(II)ArX complexes, see: ref 28g and (c) Ananikov, V. P.; Musaev, D. G.; Morokuma, K. *Eur. J. Inorg. Chem.* **2007**, 5390. (d) Ariafard, A.; Yates, B. F. *J. Organomet. Chem.* **2009**, *694*, 2075. For the effect on the overall cycle of Cu-catalyzed amide arylations, see: (e) Zhang, S.; Liu, L.; Fu, Y.; Guo, Q. *Organometallics* **2007**, *26*, 4546.

Scheme 1. Processes Examined in Our Computational Studies

(1) *barrier to oxidative addition to aryl halide*

LPd + PhX ----------→ LPd(Ph)(X)

(2) *amide binding to LPd(II)PhX*

LPd(Ph)(X) + amide ----------→ LPd(Ph)(X)amide

(3) *ligand dissociation of LPd(II)PhX*

LPd(Ph)(X) ----------→ LPd(Ph)⁺ + X⁻

(4) *formation of the κ²-bound complex*

κ¹ LPd(Ph)(amide) ----------→ κ² LPd(Ph)(amide)

(5) *barrier to reductive elimination*

LPd(Ph)(amide) ----------→ product + LPd

Ligands Examined

Xantphos, **L1**

quently used but powerful approach to understanding intricate details of critical mechanistic processes.[28a,30]

Our strategy to unraveling the structure/activity relationship of these ligands was to systematically change one portion of the ligand and calculate the effect on each step of the catalytic cycle. Scheme 1 shows the general outline of the possible steps in the catalytic cycle we would examine: oxidative addition (eq 1), associative ligand exchange (eq 2), dissociative ligand exchange (eq 3), formation of the κ²-bound amidate (eq 4), and reductive elimination (eq 5). The ligands we opted to focus on were **L1** (xantphos), **L6** (JackiePhos), **L2** (BrettPhos), **L3** (*t*-Bu₂BrettPhos), **L4** (Ph₂BrettPhos), and **L10** (a simplified version of **L8**), which are shown in Scheme 1. Xantphos was included in this comparison since it is a very effective ligand for many amidation reactions[3a−h,4a,b] and its role in Pd-catalyzed cross-couplings has never been studied computationally.[31] It also serves as a benchmark for comparison to our biarylmonophosphine ligands and to validate our computational results by further correlation with experiment. Our justification for modeling **L10** instead of **L8** rests on previous studies that demonstrate only the methyl group *ortho* to the phosphorus influences the properties of these ligands in amidation reactions.[5a]

Methods. All calculations were performed using the Gaussian '03 suite of programs,[32] primarily with Dell PowerEdge 1950 servers containing two quad-core Intel Xeon processors or Sun servers containing dual-core Opteron processors, running the sun grid engine (SGE) queuing program. We also made use of supercomputing resources for potential energy scans. Ground-state geometry optimizations were performed with the Berny

algorithm using all-atom DFT (B3LYP/6-31(d)) and the LANL2DZ basis set with the Hay−Wadt[33] effective core potential (ECP) for all Pd and Br atoms. Frequency calculations were performed on all optimized structures to confirm that the minima had no negative frequencies and transition states had a single imaginary frequency. The Gibbs free energies were calculated at 298.15 K and 1 atm. Single-point calculations were then performed with the 6-311+g(2d,p) basis set to obtain higher accuracy electronic energies. Solvation effects were calculated at the 6-311+g(2d,p) level with the CPCM method[34] in conjunction with the UAKS cavity and employing a dielectric constant of $\varepsilon = 2.374$ for toluene. Basis set superposition error (BSSE) was corrected for by use of the counterpoise method of Boys and Bernardi.[35] Although BSSE is a general phenomenon when using incomplete basis sets, correcting for it is critical when constructing potential energy diagrams.[36]

Oxidative Addition. As stated earlier, it is unlikely that oxidative addition is the rate-limiting step in most Pd-catalyzed amide arylation reactions based on previous work performed in our group.[5a] Nevertheless, the barriers for this step were calculated (Table 7), as the rate-limiting step could change for some ligands. We began by finding the barrier of oxidative addition to bromobenzene (**1-TS**, entry 1) and chlorobenzene (**2-TS**, entry 2) with xantphos·Pd (**1**). Interestingly, the geometry of these transitions states were pseudotetrahedral about the Pd center as opposed to the more common square planar conforma-

(31) For computational studies on Rh/xantphos complexes and their behavior in hydroformylation reactions, see: (a) Landis, C. R.; Uddin, J. *Dalton Trans.* **2002**, 729. (b) van der Veen, L. A.; Keeven, P. H.; Schoemaker, G. C.; Reek, J. N. H.; Kamer, P. C. J.; van Leeuwen, P. W. N. M.; Lutz, M.; Spek, A. L. *Organometallics* **2000**, *19*, 872.

(32) Frisch, M. J.; et al. *Gaussian 03*, revision D.01; Gaussian, Inc.: Wallingford, CT, 2004.

(33) Hay, P. J.; Wadt, W. R. *J. Chem. Phys.* **1985**, *82*, 299.

(34) Cossi, M.; Rega, N.; Scalmani, G.; Barone, V. *J. Comput. Chem.* **2003**, *24*, 669.

(35) Boys, S. F.; Bernardi, F. *Mol. Phys.* **1970**, *19*, 553.

(36) For instances where the correction of BSSE is important in theoretical studies of Pd-catalyzed processes, see: (a) Frankcombe, K. E.; Cavell, K. J.; Yates, B. F.; Knott, R. B. *J. Phys. Chem.* **1996**, *100*, 18363. (b) Delbecq, F.; Lapouge, C. *Organometallics* **2000**, *19*, 2716. (c) de Jong, G. T.; Sola, M.; Visscher, L.; Bickelhaupt, F. M. *J. Chem. Phys.* **2004**, *121*, 9982.

Table 7. Calculated Reaction Barriers for the Oxidative Addition of PhX with Xantphos·Pd

entry	TS	X	$\Delta G^{\ddagger}$ (kcal/mol)
1	**1-TS**	Br	26.8
2	**2-TS**	Cl	36.6

tion, probably a result of the large bite angle of xantphos.[37] Alternative transition states with *cis* or O-bound geometries could not be located. A moderate barrier of 26.8 kcal/mol was calculated for **1-TS**, but a high barrier of 36.6 kcal/mol was calculated for **2-TS**. This is consistent with the experimental observation that the use of xantphos does not allow for the Pd-catalyzed cross-coupling of unactivated aryl chlorides.[5a,38]

We found four energy minimized oxidative addition complexes for xantphos·Pd(Ph)(Br), shown in Table 8. The tetrahedral transition state **1-TS** initially leads to the highest energy tetrahedral isomer **2a** (confirmed by an IRC calculation), which then can isomerize to the lower energy *trans*[39] (**2b**), O-bound (**2c**), or *cis* (**2d**) complexes. The bond angles and bond lengths about the Pd center are listed and illustrate the large range of conformations the xantphos catalyst can adopt, underscoring the dynamic nature of this ligand. The O5–Pd–P3 bond angle of **2c** is only 76.0° while the P1–Pd–P2 bond angle ranges from 104.9° in **2d** to 113.3° in **2a** to 146.2° in **2b**.

Although aryl chlorides, triflates, and nonaflates are all capable coupling partners when using JackiePhos, we chose to focus on modeling oxidative addition with chlorobenzene as it would simplify the calculations and corresponds to the most difficult case in the series that we studied. In Table 9, the calculated barriers for oxidative addition to chlorobenzene with Pd(0) complexes of JackiePhos (entry 1), BrettPhos (entry 2), *t*-Bu₂BrettPhos (entry 3), Ph₂BrettPhos (entry 4), and **L10** (entry 5) are listed. They are quite low, even for electron-deficient ligands, ranging between 10.8 and 20.4 kcal/mol, and are in agreement with our previous computational study[29b] on the reactivity of SPhos·Pd and XPhos·Pd. The low barrier calculated for JackiePhos (20.1 kcal/mol, entry 1) supports our assertion that this step is not rate-limiting. It is interesting that even though JackiePhos is significantly more electron-deficient than xantphos, the barrier to oxidative addition of chlorobenzene with the former is over 16 kcal/mol lower in energy. This is consistent with previous findings from our laboratory concerning

the relative importance of steric and electronic factors on the rates of cross-coupling reactions.[40]

Associative Transmetalation. The step following oxidative addition is "transmetalation", in which ligand exchange of an amide for a halide probably occurs by either an associative or dissociative mechanism. Given the pK_a difference between amides (15.1 for N–H) and carbonate (10.3), we believe that deprotonation occurs following amide binding to the Lewis acidic Pd(II) center. If an associative mechanism is operative, then the amide must first bind to Pd, giving rise to a five-coordinate intermediate in the case of xantphos and a four-coordinate intermediate in the case of monophosphines, followed by deprotonation and halide dissociation. An examination of the literature reveals very few mechanistic details concerning ligand substitution with amides either experimentally or theoretically.

The amide included in our calculations was *N*-methyl acetamide, which was chosen to be representative of secondary, acyclic, alkyl amides. The calculated geometry of the four-coordinate *trans*-xantphos·Pd(Ph)(Br) complex **2b** and five-coordinate square pyramidal complex **8** with an O-bound amide are shown in Scheme 2. This binding is endothermic by 28.7 kcal/mol of energy and results in a fairly weak Pd–Br interaction in the axial position with a bond length of 3.22 Å. A similar structure with a triflate counterion could not be located.

The binding energies of *N*-methyl acetamide to each biaryl monophosphine·Pd(Ph)(Cl) complex were next determined (Table 10). We first calculated the energy of amide binding to the JackiePhos·Pd(Ph)(Cl) complex in cases where the Pd center is pointed away from the lower biaryl ring (complexes **9b–d**). The most favorable interaction, being endothermic by 18.2 kcal/mol,[41] occurred when the amide was bound to Pd through its oxygen atom and oriented *cis* to the phosphorus (**9b**). The energy of amide binding with the Pd but centered over the bottom ring was also calculated and was significantly higher in energy in both possible configurations (**9f**, 26.4 kcal/mol and **9g**, 25.1 kcal/mol). The energies of the other L·Pd(Ph)(Cl)(amide) adducts in configuration **b** were next calculated. We also verified that the lowest energy configuration for JackiePhos held for other ligands, and they did with the exception of isomer **f**. For BrettPhos and *t*-Bu₂BrettPhos, this isomer was not a stationary state, but we found that isomer **g** oriented with the amide *trans* to the phosphorus did represent a stable minimum. Larger energies for amide binding were calculated for BrettPhos- (23.0 kcal/mol, **10b**) and *t*-Bu₂BrettPhos- (23.5 kcal/mol, **11b**) ligated complexes. In contrast, with Ph₂BrettPhos, a significantly lower energy for this step (19.8 kcal/mol, **12b**) was calculated. As in the oxidative addition step, **L10** is calculated to behave similarly to JackiePhos; its oxidative addition complex requires only 17.5 kcal/mol for amide binding.

Further information on the mechanism of this step would be gained from examining transition states for amide attack and amide deprotonation. However, our efforts to locate such structures were unsuccessful, and at this point we can only qualitatively say that they will be higher in energy than the corresponding ground states.

The accessibility of isomer **b** in Table 10 relies on the free rotation about the C$_{aryl}$–P bond, which has been shown

(37) (a) Birkholz, M.-N.; Freixa, Z.; van Leeuwen, P. W. N. M. *Chem. Soc. Rev.* **2009**, *38*, 1099. (b) Kamer, P. C. J.; van Leeuwen, P. W. N. M.; Reek, J. N. H. *Acc. Chem. Res.* **2001**, *34*, 895.

(38) For the cross coupling of activated aryl chlorides using a Pd/xantphos catalyst, see: refs 6c, d and (a) Itoh, T.; Mase, T. *Org. Lett.* **2004**, *6*, 4587. (b) Patriciu, O.-I.; Finaru, A.-L.; Massip, S.; Léger, J.-M.; Jarry, C.; Guillaumet, G. *Eur. J. Org. Chem.* **2009**, 3753.

(39) Xantphos-Pd(II) complexes are often most stable as the *trans* isomer; see: ref 3b and (a) Zuideveld, M. A.; Swennenhuis, B. H. G.; Boele, M. D. K.; Guari, Y.; van Strijdonck, G. P. F.; Reek, J. N. H.; Kamer, P. C. J.; Goubitz, K.; Fraanje, J.; Lutz, M.; Spek, A. L.; van Leeuwen, P. W. N. M. *Dalton Trans.* **2002**, 2308. (b) Fujita, K.; Yamashita, M.; Puschmann, F.; Alvarez-Falcon, M. M.; Incarvito, C. D.; Hartwig, J. F. *J. Am. Chem. Soc.* **2006**, *128*, 9044.

(40) Barder, T. E.; Walker, S. D.; Martinelli, J. M; Buchwald, S. L. *J. Am. Chem. Soc.* **2005**, *127*, 4685.

(41) For experimentally determined binding energies of amines and anilines with dimeric SPhos·Pd(II)(Ar)(Cl) complexes, see: Biscoe, M. R.; Barder, T. E.; Buchwald, S. L. *Angew. Chem., Int. Ed.* **2007**, *46*, 7232.

Table 8. Xantphos·Pd(Ph)(Br) Isomers with Selected Bond Angles and Bond Lengths

2a

tetrahedral: ΔG_{rel} = +12.2 kcal/mol

Bond Angles (deg)		Bond Lengths (Å)	
P1–Pd–P3	113.3	P1–Pd	2.55
P1–Pd–C2	102.6	C2–Pd	1.98
C2–Pd–P3	102.7	P3–Pd	2.55
P3–Pd–Br4	119.8	Br4–Pd	2.62
Br4–Pd–P1	119.7	O5–Pd	3.17
C2–Pd–Br4	92.2		

2b

*xanthene backbone removed for clarity

trans: ΔG_{rel} = 0 kcal/mol

Bond Angles (deg)		Bond Lengths (Å)	
P1–Pd–P3	146.2	P1–Pd	2.38
P1–Pd–C2	92.5	C2–Pd	2.03
C2–Pd–P3	92.5	P3–Pd	2.38
P3–Pd–Br4	91.0	Br4–Pd	2.68
Br4–Pd–P1	91.0		
C2–Pd–Br4	167.7		

2c

O-bound: ΔG_{rel} = +4.0 kcal/mol

Bond Angles (deg)		Bond Lengths (Å)	
P3–Pd–C2	94.8	P1–Pd	3.27
C2–Pd–Br	92.4	C2–Pd	1.99
Br–Pd–O5	97.6	P3–Pd	2.33
O5–Pd–P3	76.0	Br4–Pd	2.57
Br4–Pd–P3	161.2	O5–Pd	2.49
O5–Pd–C2	169.9		

2d

cis: ΔG_{rel} = +2.1 kcal/mol

Bond Angles (deg)		Bond Lengths (Å)	
P1–Pd–P3	104.9	P1–Pd	2.42
P1–Pd–C2	89.3	C2–Pd	2.02
C2–Pd–Br4	83.6	P3–Pd	2.64
P3–Pd–Br4	86.5	Br4–Pd	2.60
Br4–Pd–P1	155.8	O5–Pd	3.59
C2–Pd–P3	163.7		

Table 9. Calculated Reaction Barriers for the Oxidative Addition of PhCl with L_1Pd
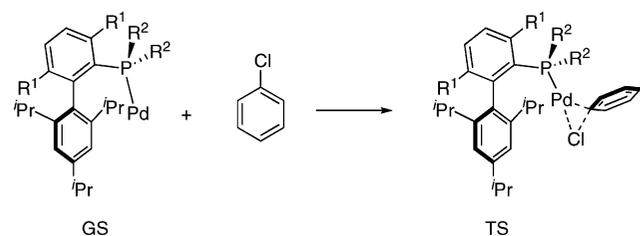
entry	GS	TS	R^1	R^2	$\Delta G^{\ddagger}$ (kcal/mol)
1	**3**	**3-TS**	2,5-OMe	3,5-CF₃Ph	20.1
2	**4**	**4-TS**	2,5-OMe	Cy	10.8
3	**5**	**5-TS**	2,5-OMe	t-Bu	20.1
4	**6**	**6-TS**	2,5-OMe	Ph	16.5
5	**7**	**7-TS**	2-Me	3,5-CF₃Ph	20.4

in previous computational studies to be quite difficult for Me₄t-Bu₂XPhos·Pd(Ph)(amidate).[5a] The JackiePhos·Pd(Ph)-(amidate) complex is likely to have a lower barrier of rotation for two reasons: first, the methoxy group *ortho* to phosphorus is smaller than the methyl group in Me₄t-Bu₂XPhos, and second, the P-bound arenes of JackiePhos are much smaller than the bulky t-Bu groups of Me₄t-Bu₂XPhos. To support this assertion, we performed a potential energy scan about the C_{aryl}–P bond in which a restricted structure optimization was executed at every 10°. We chose to calculate this with the JackiePhos·Pd(Ph)(amidate) complex because it, too, would need to freely rotate once formed and, being larger

than the chloride complex, would be the more difficult case. The maximum of the resulting energy curve, shown in Figure 2, corresponds to a barrier of rotation of 19.8 kcal/mol, an amount of energy that is readily overcome even at room temperature.

We next performed potential energy scans about the C2–P3 bond with analogous complexes containing the other ligands, and very similar curves were obtained (not shown). However, the maximum for the BrettPhos complex lies at a dihedral angle of 90° while all of the other ligands gave maxima at 80°. The barrier heights for these complexes are listed in Table 11: JackiePhos (entry 1), BrettPhos (entry 2), and Ph₂BrettPhos (entry 4) give barriers of very similar energies (19.2, 20.5, and 19.1 kcal/mol, respectively). Of note is that switching the methoxy group of the upper ring to a methyl group in JackiePhos increases the barrier significantly to 23.3 kcal/mol (entry 5), presumably because of its larger size. We also found that the barrier to rotation for the most sterically congested ligand, t-Bu₂BrettPhos (entry 3), is only 27.7 kcal/mol (compared to 33 kcal/mol for Me₄t-Bu₂XPhos[5a]). It follows from the Eyring equation that this barrier corresponds to a half-life of only 9.16 min at 110 °C assuming a first-order rate law. Based on these data, we conclude that under the reaction conditions (110–130 °C) all the ligands including t-Bu₂BrettPhos can freely rotate with the Pd moiety being either over or away from the lower biaryl ring.

Dissociative Transmetalation. The loss of a halide/pseudohalide to form cationic Pd(II) intermediates is quite common

Scheme 2. Calculated Binding Energy of *N*-Methyl Acetamide to Xantphos·Pd(Ph)(Br)
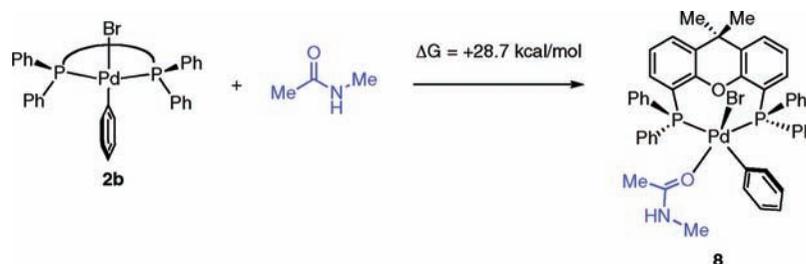
Table 10. Calculated Binding Energies of *N*-Methyl Acetamide to L_1·Pd(Ph)(Cl)[a]

complex	R^1	R^2	ΔG (kcal/mol)					
			b	c	d	e	f	g
9	2,5-OMe	3,5-CF₃Ph	18.2	18.5	27.4	33.6	26.4	25.1
10	2,5-OMe	Cy	23.0					30.1
11	2,5-OMe	*t*-Bu	23.5					37.4
12	2,5-OMe	Ph	19.8					
13	2-Me	3,5-CF₃Ph	17.5					

[a] ΔG_{rel} is in reference to isomer **a** of each complex and *N*-methyl acetamide.

in Heck-type processes[42] but is not necessary for most cross-coupling reactions in which an organometallic component participates as the nucleophile. However, this pathway should be considered for reactions involving weakly nucleophilic, nonmetallic partners, such as hindered amides. Furthermore, dissociative ligand exchange through a cationic Pd(II) intermediate has been suggested by van Leeuwen to occur for xantphos-Pd(II) complexes undergoing *cis/trans* isomerization[39a] and in the amination of aryl triflates.[43]

For the following calculations, we deemed it important to model both the bromide and triflate, as the latter are so much more effective as leaving groups.[44] It was critical for the inclusion of solvation effects for this step as dissociation was

highly endothermic in the gas phase. As depicted in Table 12, the energy differences between cationic complex **14** and both the *trans*-xantphos·Pd(Ph)(Br) (**2b**) and *trans*-xantphos·Pd(Ph)(OTf) (**15**) complexes were determined. The loss of the bromide is endothermic by 17.5 kcal/mol, but loss of triflate is endothermic by only 0.8 kcal/mol. It should be pointed out that correction for BSSE was critical for Br dissociation as it was originally in error by 16.5 kcal/mol, while triflate dissociation was only in error by 3.2 kcal/mol (a more typical value). The unusually large error in the first case is likely a result of the use of the approximations implicit in the LANL2DZ basis set for an entire fragment.[45]

The ionization energy requirement for the bromide complex could be low enough to outcompete the associative pathway. For aryl triflates, the nearly equal energies of **14** and **15**, our inability to locate a five-coordinate amide-bound Pd-triflate complex, and structural characterization by van Leeuwen[39a] of a cationic xantphos·Pd(Ar)(OTf) complex are good evidence

(42) (a) Deeth, R. J.; Smith, A.; Brown, J. M. *J. Am. Chem. Soc.* **2004**, *126*, 7144, references cited therein. (b) Tanaka, D.; Romeril, S. P.; Myers, A. G. *J. Am. Chem. Soc.* **2005**, *127*, 10323.

(43) Guari, Y.; van Strijdonck, G. P. F.; Boele, M. D. K.; Reek, J. N. H.; Kamer, P. C. J.; van Leeuwen, P. W. N. M. *Chem.—Eur. J.* **2001**, *7*, 475.

(44) Howells, R. D.; McCown, J. D. *Chem. Rev.* **1977**, *77*, 69.

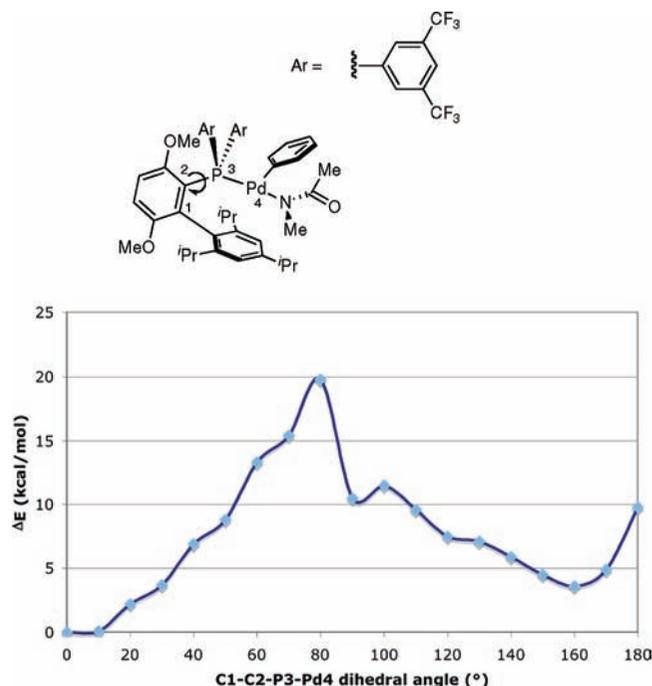(45) Wadt, W. R.; Hay, J. J. *J. Chem. Phys.* **1985**, *82*, 284.

Figure 2. Potential energy scan for rotation about the C2−P3 bond.

Table 11. Barriers to Rotation About the C2−P3 Bond for each L₁Pd(Ph)(amidate) Complex

entry	ligand	maxima (deg)	ΔG^a (kcal/mol)
1	JackiePhos	80	19.2
2	BrettPhos	90	20.5
3	*t*-Bu₂BrettPhos	80	27.7
4	Ph₂BrettPhos	80	19.1
5	**L10**	80	23.3

a The electronic energies of structures corresponding to the indicated dihedral angle were recalculated at 6-311+g(2d,p) with CPCM solvation correction and zero-point energy correction.

that ligand exchange occurs by a dissociative pathway. However, based on the experimental results that more hindered amides (e.g., those that are the focus of this paper) are not readily arylated with a xantphos/Pd catalyst and reductive elimination should not be difficult (*vide infra*), we must conclude that there is also a significant energy cost to the approach of the amide and/or isomerization from O- to N-bound isomers.

With a handle on the difference in energy for ionization in xantphos·Pd(Ph)(OTf/Br) complexes, we were prompted to perform similar calculations on the JackiePhos·Pd(Ph)(OTf/Cl) complexes (Table 13). The empty coordination site in the cationic product may be *cis* or *trans* to the phosphorus, but structures in which the empty site is *trans* to the phosphorus were much lower in energy and are the only ones considered here. Additionally, the Pd may be pointed away from the bottom ring, in which it has a dative bond with the oxygen, or toward the lower ring, in which it interacts with the π-electrons of the arene. Surprisingly, C-bound isomer **18** is significantly lower in energy than O-bound isomer **17**. Unlike the xantphos system, however, ionization of both the chloride (42.9 kcal/mol to reach **18**) and triflate (34.9 kcal/mol to reach **18**) were prohibitively high in energy. The resistance to ionization of the JackiePhos system is probably a consequence of the Pd being both coordinatively unsaturated and electron poor.

κ^2-**Binding of the Amide to Pd.** Previous work has demonstrated that Pd-catalyzed amidation reactions are complicated by the formation of κ^2-amidate complexes in which the amide is simultaneously bound to the palladium center at both the nitrogen and oxygen atoms.[39b] In these studies, it was shown that κ^2-amidate complexes do not undergo reductive elimination as readily as κ^1-amidate complexes. While some monophosphine ligands may not be effective ligands for amidation as they allow κ^2-amidate formation, we have previously shown that bulky monodentate biaryl phosphines can form effective catalysts for amidation.[4c,5] In light of the experimental evidence presented,[39b] suggesting that catalyst inhibition and inactivation results from κ^2-binding, we calculated the relative energies of κ^1- and κ^2-bound isomers of both xantphos·Pd(Ph)(amidate) and JackiePhos·Pd(Ph)-(amidate) complexes. Quite unexpectedly, the κ^2-bound xantphos structure (**20**) is calculated to be lower in energy than the *cis*-κ^1-bound structure (**19**) by 9.3 kcal/mol (Scheme 3). This energy is seemingly in disagreement with the previously reported IR and NMR data obtained for xantphos·(Ph)(*N*-phenylacetamide) complexes that support κ^1-bound structures as being more stable.[39b] However, the amide-bound complexes in this study were prepared by the addition of potassium amides to xantphos·Pd(Ph)(Br) at room temperature, and the thermodynamically more stable isomer may have not been kinetically accessible. Similarly, JackiePhos·Pd(Ph)(amidate) favors κ^2-bound structures, pointed both toward (**22**, −2.3 kcal/mol) and away (**23**, −3.7 kcal/mol) from the lower biaryl ring (Scheme 4). In contrast to the xantphos system, the barrier to reach these structures is probably not as high since there is an open coordination site on Pd. Based on these results, we believe κ^2-binding does not necessarily lead to decomposition or inhibit catalysis (i.e., it can form reversibly), but rather, it may lie on the path to catalyst decomposition for unhindered monodentate ligands.
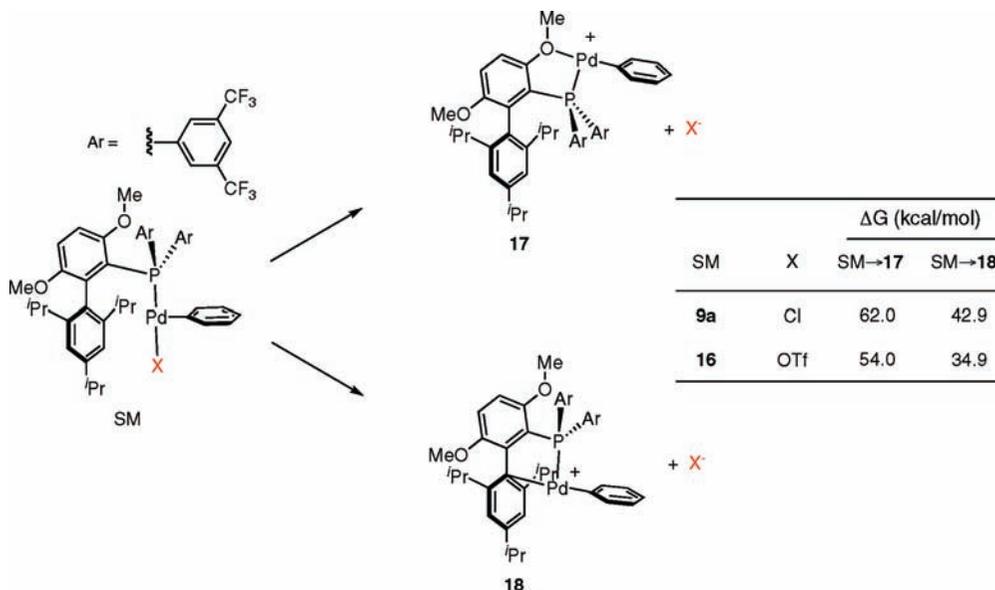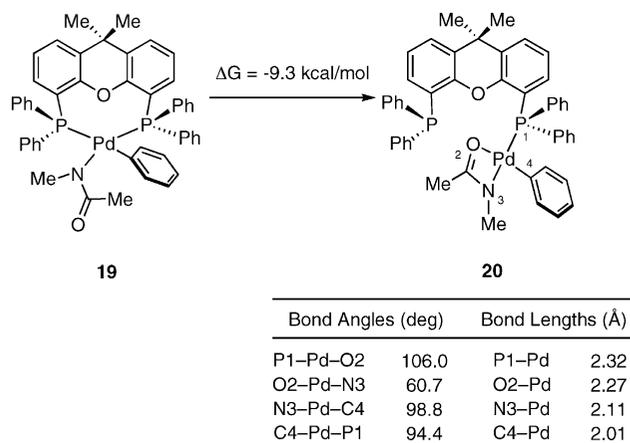
Reductive Elimination. Reductive elimination is often the most difficult step for the arylation of weaker nucleophiles such as amides.[46] We first calculated the barrier for C−N bond formation from the xantphos·Pd(Ph)(amidate) complex and found it was 20.4 kcal/mol (**8-TS,** Scheme 5). In contrast to the tetrahedral geometry in the transition state for oxidative addition, this geometry is square planar, proceeding from *cis*-complex **19**. We believe that a tetrahedral transition state similar in geometry to those found for oxidative addition (Table 7) is no longer accessible due to the larger size of the amide compared to bromide.

Next, we compared the barrier to C−N bond formation for each of the biaryl monophosphine ligands (Table 14).[47] The ligands that allowed for the lowest barriers of reductive elimination (16.6 kcal/mol for both) were *t*-Bu₂BrettPhos (**11-TS,** entry 2) and **L10** (**13-TS,** entry 5), while the barrier for this step was slightly higher with JackiePhos (17.7 kcal/mol, entry 1). Both BrettPhos and Ph₂BrettPhos were predicted to be less effective at promoting this step, with barriers of 19.7 (entry 2) and 20.0 kcal/mol (entry 4), respectively.

Five-membered cyclic transition states were also found in which an O-bound amidate pivots back toward the reactive Ph group to form a C−N bond (Figure 3). In both the case of xantphos (**14-TS**, 23.0 kcal/mol) and JackiePhos (**15-TS**, 22.0 kcal/mol), this transition state was higher in energy, leading us

(46) Hartwig, J. F. *Inorg. Chem.* **2007**, *46*, 1936.
(47) For a computational study on the reductive elimination of aryl amines from biaryl monophosphine arylpalladium amido complexes, see: Barder, T. E.; Buchwald, S. L. *J. Am. Chem. Soc.* **2007**, *129*, 12003.

Table 12. Dissociative Mechanism for Xantphos·Pd(Ph)(X)

X	GS	ΔG (kcal/mol)
Br	**2b**	17.5
OTf	**15**	0.8
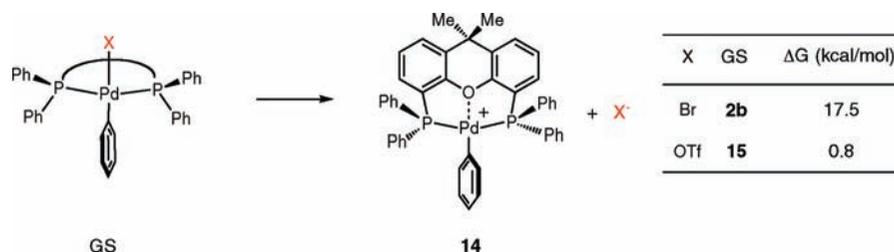
Table 13. Dissociative Mechanism for JackiePhos·Pd(Ph)(X)

		ΔG (kcal/mol)	
SM	X	SM→**17**	SM→**18**
9a	Cl	62.0	42.9
16	OTf	54.0	34.9

Scheme 3. Calculated Energy for κ²-Binding of Xantphos·Pd(Ph)(Amidate)

ΔG = -9.3 kcal/mol

| Bond Angles (deg)		Bond Lengths (Å)	
P1–Pd–O2	106.0	P1–Pd	2.32
O2–Pd–N3	60.7	O2–Pd	2.27
N3–Pd–C4	98.8	N3–Pd	2.11
C4–Pd–P1	94.4	C4–Pd	2.01

to believe that it constitutes a minor pathway for this reaction. However, it may be more important in the arylation of other less hindered amides or if O to N isomerization proves difficult.

Catalytic Cycle. Without an analysis of a continuous potential energy diagram for the catalytic cycle, the relative contributions from each mechanistic step are not entirely clear. Accordingly, the relative energies of each step through the amide binding event were connected in Figures 4 and 5 so that such an analysis could be performed. We did not construct a potential energy diagram for the entire catalytic cycle because of the uncertainties in the barriers to trans-

metalation as well as the energy change for salt precipitation and dissolution, as this is a heterogeneous reaction.

First, in Figure 4, the potential energy diagram for the xantphos-Pd catalyst is depicted. Although aryl triflates likely react through a dissociative pathway, we will examine the energy pathway for the aryl bromide case because it will be more comparable to the mechanism involving the biaryl-monophosphine-derived catalysts. In the catalytic cycle with bromobenzene, oxidative addition is slightly endothermic by +3.3 kcal/mol based on the difference between **1** with bromobenzene and the most stable *trans*-xantphos-Pd(II) isomer (**2b**). Assuming transmetalation operates by associative ligand exchange, amide binding (**8**) brings the total energy needed to 32.0 kcal/mol.

The information contained in the potential energy diagram of the biarylmonophosphine-Pd catalysts in Figure 5 is not as readily apparent as in Figure 4. First, the thermodynamics of oxidative addition to reach **C** is drastically different for each catalyst, all being exothermic but with an energy change ranging between −0.2 and −13.8 kcal/mol. As a consequence, the more exothermic this step becomes, the more energy that will be required to scale the subsequent reaction barriers. In this scenario, the energy requirement for catalysis will not be the energy change from starting materials to the highest barrier but the difference between the lowest point (**C**) and the highest barrier. In the cases of *t*-Bu₂BrettPhos and **L10**, the energy for bond rotation (**D**) is the highest peak in Figure 5, but we believe

Scheme 4. Calculated Energies of κ^2-Binding of JackiePhos·Pd(Ph)(Amidate)

21

Pd-down

$\Delta G_{rel} = 0$ kcal/mol

22

κ^2-**Pd-down**

-2.3 kcal/mol

23

κ^2-**Pd-away**
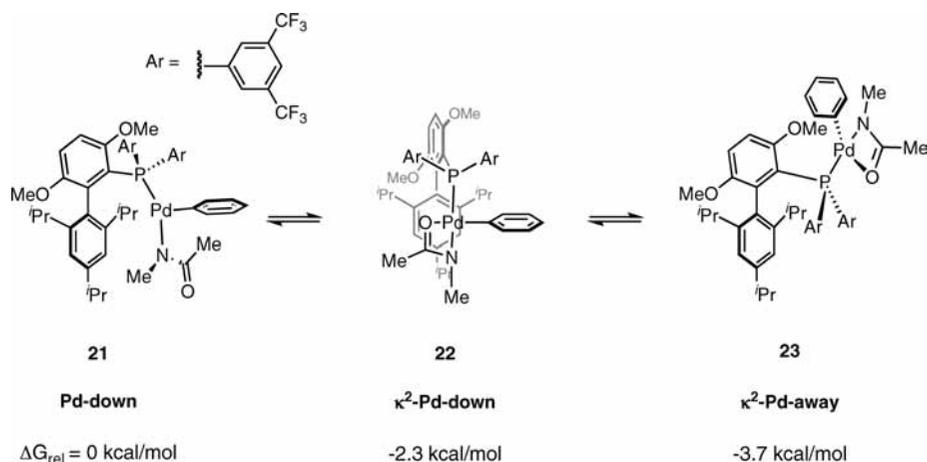
-3.7 kcal/mol

Scheme 5. Calculated Barrier for Reductive Elimination of *cis*-Xantphos·Pd(Ph)(Amidate)

19

$\Delta G^{\ddagger} = 20.4$ kcal/mol

8-TS
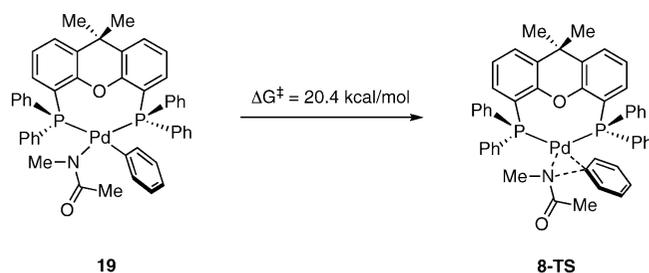
Table 14. Calculated Barriers for Reductive Elimination of L_1·Pd(Ph)(Amidate)

GS

TS

entry	GS	TS	R^1	R^2	$\Delta G^{\ddagger}$ (kcal/mol)
1	**21**	**9-TS**	2,5-OMe	3,5-CF$_3$Ph	17.7
2	**24**	**10-TS**	2,5-OMe	Cy	19.7
3	**25**	**11-TS**	2,5-OMe	*t*-Bu	16.6
4	**26**	**12-TS**	2,5-OMe	Ph	20.0
5	**27**	**13-TS**	2-Me	3,5-CF$_3$Ph	16.6

that with consideration of the barriers for transmetalation and reductive elimination it will not be rate-limiting.

Although we lack the information to give predicted energy requirements and overall rates for each catalyst, we find that the energy differences from the lowest energy point and the amide-bound complex correlate well with ligand performance in most cases. These energies are listed in Table 15, and the smallest energy requirement is associated with JackiePhos (18.2 kcal/mol) and **L10** (17.5 kcal/mol). We feel that the trends shown here will be consistent but amplified when considering the barriers for amide attack and deprotonation. Since **L10** is calculated to perform equally well or better than JackiePhos in each mechanistic step but is completely ineffective in promoting the reaction, we believe the catalyst formed from it is not stable

under the reaction conditions, degrading by an as yet undetermined pathway.

Conclusions

In summary, we have reported an efficient method for the N-arylation of acyclic secondary amides with aryl nonaflates, triflates, and chlorides. The catalyst system is also useful for the N-arylation secondary carbamates, ureas, and sulfonamides and the diarylation of primary amides. A ligand for this transformation, JackiePhos (**L6**), was designed based on the knowledge that "transmetalation" was rate-limiting for the arylation of primary amides and the hypothesis that a more electrophilic and less sterically demanding Pd(II) intermediate would facilitate the "transmetalation" of secondary amides. Our synthetic, mechanistic, and computational studies showed the success of JackiePhos is due to (1) the methoxy group *ortho* to the phosphorus and (2) the strongly electron-withdrawing P-bound 3,5-(bis)trifluoromethylphenyl groups.

Theoretical studies have provided insight into the mechanism of "transmetalation" and show that the lowest energy conformation for amide binding occurs while Pd is pointed away from the lower biaryl ring. A potential energy scan about the $C_{aryl}-P$ bond indicates that this conformation, in which Pd interacts with the methoxy group *ortho* to the phosphorus, is quite accessible. Our synthetic studies show that the *ortho* methoxy group is critical for catalyst stability and cannot be removed or substituted with a methyl group. Additionally, computational studies predict the most favorable energies of amide binding for ligands containing the highly electron-withdrawing P-bound 3,5-(bis)-trifluoromethylphenyl groups. Overall, it seems the "transmetalation" of secondary amides is facilitated by the ability of the ligand to access a highly electrophilic Pd(II) intermediate where

14-TS

23.0 kcal/mol

15-TS

22.0 kcal/mol
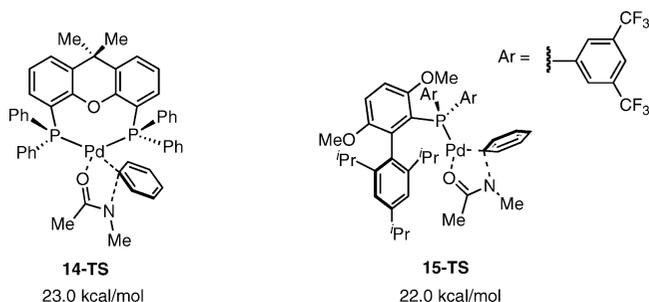
Figure 3. Five-membered cyclic transition states for reductive elimination.
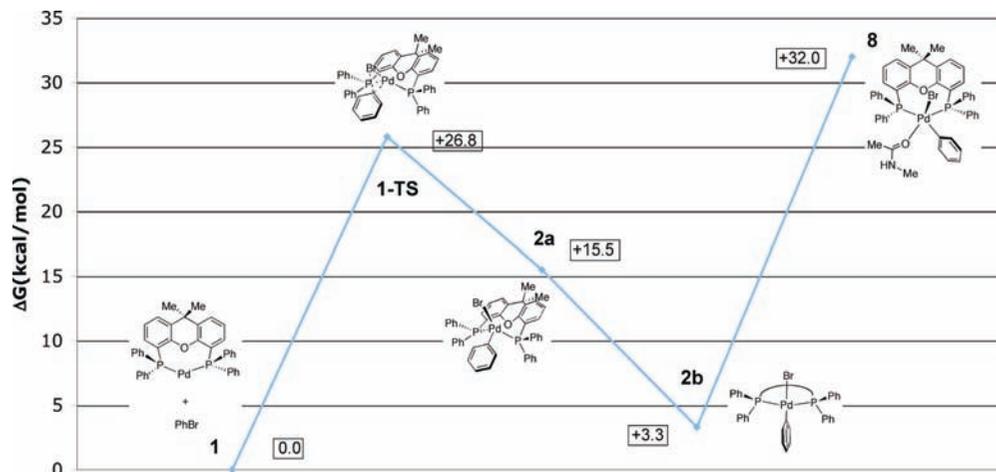
Figure 4. Partial potential energy diagram of the catalytic cycle with the xantphos-Pd catalyst.
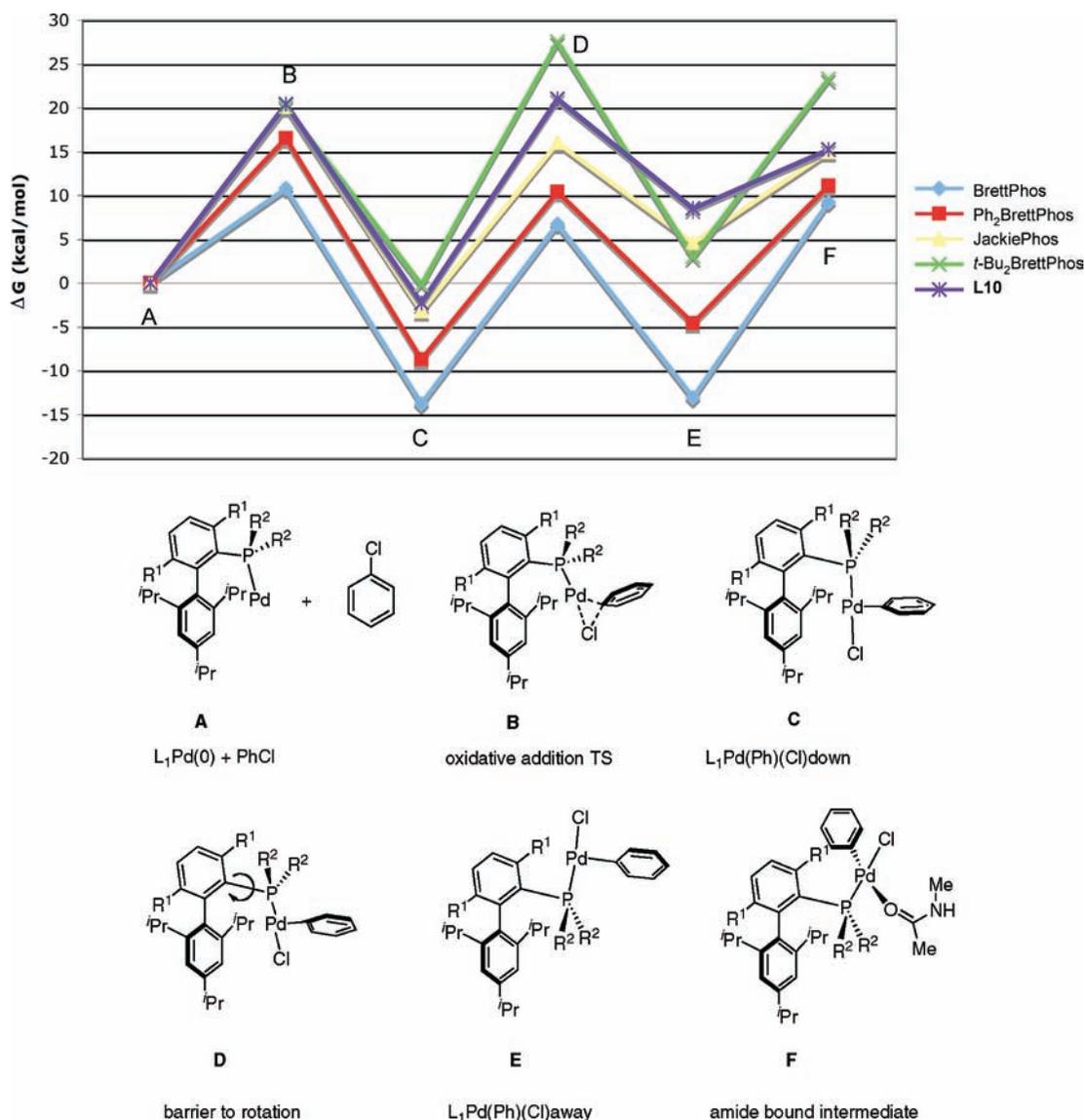

Figure 5. Partial potential energy diagram of the catalytic cycle with biarylmonophosphine-Pd catalysts.

the Pd is oriented away from the bottom ring of the biaryl backbone and stabilized by the *ortho* methoxy group. Additionally, the barrier to reductive elimination was lower for the electron-deficient JackiePhos compared to other sterically similar

ligands (Ph$_2$BrettPhos, **L4**). However, there remain many questions on the precise mechanism and energetic requirements of the transmetalation step, preventing the construction of a full potential energy diagram. Overall, these studies further expand

Table 15. Calculated Energy Required for Catalytic Cycle through Amide Binding (Not Including Deprotonation or Reductive Elimination)

ligand	ΔG (kcal/mol)
xantphos	32.0[a]
JackiePhos	18.2[b]
BrettPhos	23.0[b]
t-Bu$_2$BrettPhos	23.5[b]
Ph$_2$BrettPhos	19.8[b]
L10	17.5[b]

[a] Difference in energy from lowest energy state (**1**) and amide binding (**8**) in Figure 4. [b] Difference in energy from lowest energy state (**C**) and amide binding (**E**) in Figure 5.

our understanding of structural features of biarylmonophosphine ligands and how each of these contributes to the catalysts derived from them.

Supporting Information Available: Experimental procedures and spectral data for all compounds, computational data, kinetic plots, and complete ref 32. This material is available free of charge via the Internet at http://pubs.acs.org.

JA9044357